

## Universal critical amplitude ratios in CHF<sub>3</sub>

Ulrike Narger and David A. Balzarini

*Department of Physics, University of British Columbia, Vancouver, British Columbia, Canada V6T 2A6*

(Received 13 September 1988; revised manuscript received 18 January 1989)

We have performed experiments on fluoroform close to its critical point, using an optical interference technique which is virtually free of gravity effects. Data were obtained in the temperature range  $-4 \times 10^{-2} < t < 3 \times 10^{-4}$ , where  $t = (T - T_c)/T_c$  is the reduced temperature. The width of the coexistence curve, the compressibility on the critical isochore, and the chemical potential along the critical isotherm were simultaneously measured in the same experiment in an effort to ensure self-consistency of the results. We analyzed the data using critical power laws and incorporating wherever necessary corrections to scaling to obtain values for the critical exponents and amplitudes. We compare our results with theory and with previous experimental data.

### I. INTRODUCTION

Near a critical point, various thermodynamic quantities along special thermodynamic paths behave as power laws with critical exponents which, according to the universality hypothesis, depend only on the symmetry of the Hamiltonian and the dimensionality of the system, not the specifics of the interaction. This implies that all systems belonging to the same universality class should exhibit the same critical exponents. Fluids near the gas-liquid critical point fall into the universality class of three-dimensional Ising-like systems.

In a pure fluid, the order parameter is related to the density difference  $\rho_l - \rho_v$  between the liquid and vapor phases and behaves asymptotically as

$$\Delta\rho = \frac{\rho_l - \rho_v}{2\rho_c} = B_0(-t)^\beta, \quad (1)$$

where  $\rho_c$  is the critical density and  $t = (T - T_c)/T_c$  the reduced temperature.  $B_0$  is a system-dependent critical amplitude.

Similarly, the isothermal compressibility  $\kappa_T^+$  ( $\kappa_T^-$ ) above (below) the critical point diverges with an exponent  $\gamma^+$  ( $\gamma^-$ ) as

$$\kappa_T^\pm = \frac{P_c}{\rho_c^2} \left[ \frac{\partial \rho}{\partial \mu} \right]_T = \Gamma_0^\pm (\mp t)^{-\gamma^\pm}, \quad (2)$$

where  $\mu$  is the chemical potential,  $P_c$  is the critical pressure, and  $\Gamma_0^+$  ( $\Gamma_0^-$ ) is the nonuniversal critical amplitude above (below) the critical point.

Along the critical isotherm, the deviation  $\Delta\mu$  of the chemical potential from its value at the critical point  $\mu_c$  is expected to scale with the exponent  $\delta$  as

$$\Delta\mu = \frac{\mu - \mu_c}{\mu_c} = D_0 \Delta\rho^* |\Delta\rho^*|^{\delta-1}. \quad (3)$$

Here,  $\Delta\rho^* = (\rho - \rho_c)/\rho_c$  is the dimensionless density difference from the critical density and  $D_0$  is another system-dependent amplitude.

The exponents  $\beta$ ,  $\gamma$ , and  $\delta$  have been calculated for the three-dimensional Ising model both by high-temperature series expansions<sup>1,2</sup> and  $\epsilon$  expansions.<sup>3,4</sup> Recent results obtained by these methods agree well and furnish values of  $\beta = 0.325 - 0.327$ ,  $\gamma^+ = \gamma^- = 1.237 = 1.241$ . Given  $\beta$  and  $\gamma^\pm$ ,  $\delta$  can be calculated from the scaling relation  $\gamma^+ = \gamma^- = \beta(\delta - 1)$ . One obtains  $\delta$  to be between 4.79 and 4.82.<sup>5</sup>

The power laws for  $\Delta\rho$ ,  $\kappa_T^\pm$ , and  $\Delta\mu$  given above are exact only asymptotically close to the critical point. For pure fluids, this asymptotic region is very small.<sup>6</sup> Therefore, for data taken at larger distances from the critical point, contributions from the "irrelevant" operators to the energy density have to be taken into account by including correction to scaling terms.<sup>7</sup> For example, the order parameter should be fitted to a function of the form

$$\Delta\rho = B_0(-t)^\beta [1 + B_1(-t)^{\Delta_1} + B_2(-t)^{\Delta_2} + \dots], \quad (4)$$

where  $\Delta_1$  and  $\Delta_2$  are universal correction to scaling exponents.  $\Delta_1$  has been calculated by high-temperature expansion, giving values of  $\Delta_1 = 0.49 \pm 0.08$ ,<sup>8</sup>  $0.54 \pm 0.05$ ,<sup>2</sup> and  $0.50 \pm 0.03$ ,<sup>1</sup> and from renormalization group calculations<sup>3</sup> which find  $\Delta_1 = 0.493 \pm 0.007$ .  $\Delta_2$  is usually approximated by  $\Delta_2 \approx 2\Delta_1$ .<sup>5</sup>  $B_1$  and  $B_2$  are nonuniversal correction to scaling amplitudes.

The exponents  $\beta$ ,  $\gamma^\pm$ , and  $\delta$  are related by a scaling law,  $\gamma = \beta(\delta - 1)$ .<sup>9</sup> Scaling also predicts that, even though the individual critical amplitudes are system dependent, certain combinations of them are universal, for example, the ratios  $\Gamma_0^+/\Gamma_0^-$  and  $D_0\Gamma_0^+B_0^{\delta-1}$  are expected to be system independent.

Measurements of these amplitude ratios have been reported earlier.<sup>10,11</sup> In these publications, results obtained by different experimental techniques were combined to determine the amplitude ratios. This method, however, is subject to errors due to the different data evaluation methods used in the different experiments and, in particular, susceptible to effects caused by different determinations of the critical temperatures, which affect the critical amplitude ratios considerably. For a consistent determination of the amplitude ratios, all of the amplitudes

should therefore be extracted from a single experiment. In this way, the critical temperature can be determined independently in the evaluation of the various quantities, and agreement is an important check on the consistency of the results.

This approach was followed by Weber<sup>12</sup> and later improved by Pestak and Chan<sup>13,14</sup> who used a stack of capacitor plates to measure the density as a function of chemical potential in Ne, N<sub>2</sub>, and HD. Their results are very self-consistent and show good agreement with theory. However, close to the critical point, their data are affected by gravitational rounding which they correct for by analyzing their data using the restricted cubic model.<sup>15,16</sup>

In order to minimize gravitational rounding, we used an optical interference technique which is less susceptible to gravitational rounding effects.<sup>17</sup> Like the capacitor method, it allows measurements of the coexistence curve, compressibility, and critical isotherm in a single experiment. By confining the sample to a thin cell, gravity effects can be minimized even close to the critical point, so that no corrections due to beam bending have to be made. We used a cell only 1.86 mm thick, which enables us to approach the critical point as close as  $|t| \approx 10^{-6}$  without encountering appreciable errors due to gravitational rounding. For measurements on the critical isotherm, only reduced densities  $\Delta\rho^* > 4 \times 10^{-4}$  were used for the evaluation, for which beam bending errors are less than 0.1%.

The remainder of this paper is organized as follows. Section II describes the experimental method. Section III discusses the results of the coexistence curve, compressibility, and critical isotherm, and Sec. IV presents the results of the amplitude ratios and compares them with theoretically predicted values and the results of other experiments.<sup>13</sup>

## II. EXPERIMENTAL

The experiments were carried out on fluoroform (Freon 23, CHF<sub>3</sub>), which has its liquid-gas critical point at the pressure  $P_c \approx 4.75$  MPa, temperature  $T_c \approx 26.0^\circ\text{C}$ , and density  $\rho_c = 0.527$  g/cm<sup>3</sup>. The gas was obtained from Matheson Gas Products and had a purity of 98%, as specified by the supplier.

An optical sample cell with parallel sapphire windows spaced  $1.86 \pm 0.01$  mm apart was filled with fluoroform at an average density as close to  $\rho_c$  as possible. The deviation from critical filling can be estimated by observing the rise or fall of the meniscus between the liquid and vapor phase as the critical point is approached. Our cell was slightly overfilled, the deviation from critical density being less than 0.1%.

The cell was placed into a two-stage thermostat which controlled the temperature to an accuracy of  $\pm 0.2$  mK. Its temperature was measured by an HP 2804A quartz thermometer, the probe of which was embedded in the innermost heating stage of the thermostat. Inside the cell, the fluid is compressed under its own weight, the density at the bottom being larger than the critical density, and at the top, lower. This leads to an equilibrium

density profile  $\rho(z)$ . The density  $\rho$  is related to the refractive index  $n$  via the Lorenz-Lorentz relation

$$\rho = \frac{1}{\mathcal{L}} \frac{(n^2 - 1)}{(n^2 + 2)}. \quad (5)$$

Here,  $\mathcal{L}$  is the Lorenz-Lorentz function which depends, in general, on density and temperature.  $\mathcal{L}$  has been measured for fluoroform in our laboratory by recording, for a given density, the corresponding refractive index in the one-phase region close to the coexistence curve. The results of this experiment will be published elsewhere.<sup>18</sup>

The variation of density with height within the cell is accompanied by a variation of refractive index with height. Thus from a measurement of refractive index the density can be directly inferred.

The experimental setup is shown in Fig. 1. The light source was a 5-mW He-Ne laser with wavelength  $\lambda$  of 6328 Å, rendered uniphase by a spatial filter and then collimated into a parallel beam of diameter 2.5 cm. Two polarizers reduced its intensity to minimize optical heating of the sample. The cell is placed in a Mach-Zehnder interferometer. A beam splitter divides the incoming beam into a "sample beam" traversing the sample and a reference beam. Coherent light passing through the sample at different heights experiences different phase shifts, depending on the local refractive index at that height. Upon recombining the "sample beam" with the reference beam, an interference pattern is observed. The fringes in this pattern vary with the temperature of the sample. This interferogram is recorded by a slit camera with continual film transport in the image plane of a focusing lens.<sup>19</sup> As the cell temperature is varied, the density profile within the cell changes, leading to a change in the interference pattern. By recording the interferogram as a function of temperature, one can deduce the temperature dependence of the density profile, and obtain information on the order parameter along the coexistence curve, the compressibility close to  $T_c$ , and the critical isotherm, all from the same experiment. In this way, self-consistency of the results can be achieved.

As our cell had such a small path length (1.86 mm), gravity effects can be neglected: at reduced temperatures as small as  $(T - T_c)/T_c = -2 \times 10^{-6}$ , gravitational rounding introduces an error of only about  $\frac{1}{5}$  fringe close to the meniscus, which is smaller than the accuracy with which fringes can be counted close to the critical point.

A listing of the experimental data used in this publication is available from the AIP.<sup>20</sup>

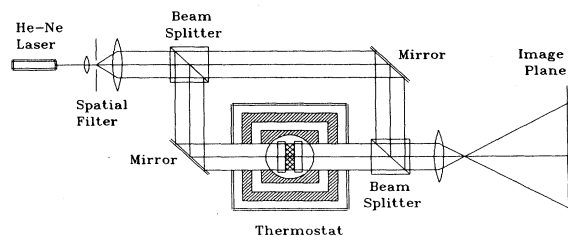


FIG. 1. Experimental setup.

### III. RESULTS

#### A. Order parameter

Below  $T_c$ , as the temperature is lowered, the density difference between liquid and vapor phases increases, causing interference fringes to “disappear” into the image of the meniscus. The order parameter can be obtained by counting, as a function of temperature, the number of “missing” fringes on both the liquid and vapor side of the meniscus. These numbers are related, through the Lorenz-Lorentz relation, to the density differences  $\rho_l - \rho_c$  and  $\rho_c - \rho_v$ , respectively. Their sum is therefore proportional to the order parameter  $\Delta\rho = (\rho_l - \rho_v)/2\rho_c$ . Data have been taken in the reduced temperature interval  $10^{-6} < -t < 4.2 \times 10^{-2}$ . Table I shows the results of various fits of the data to the expression

$$\Delta\rho = B_0(-t)^\beta [1 + B_1(-t)^\Delta + B_2(-t)^{2\Delta} + B_3(-t)^{3\Delta}] \quad (6)$$

The first fits in the table were performed on data in the temperature range  $-t \leq 10^{-4}$ , in which only one correction to scaling term has been taken into account and higher-order terms are assumed negligible. Fits over the entire temperature range, using two correction to scaling terms, favor a value of  $\beta = 0.331$  which is slightly higher than the theoretical value ( $\beta = 0.325 - 0.327$ ). Adding the third correction term, we obtain  $\beta = 0.3289$ , very close to the predicted value. Figure 2 shows the data (640 points from four individual runs). In this plot, the leading temperature dependence has been divided out, and  $\log_{10}[\Delta\rho/(-t)^\beta]$  is plotted versus  $(-t)$ .

#### B. Compressibility

The chemical potential  $\Delta\mu$ , as measured from the meniscus, is related to the height  $\Delta z$  in the cell via the relation  $\Delta\mu = g \Delta z$ . Thus, the compressibility at constant temperature  $\kappa_T^\pm$ ,

$$\kappa_T^\pm = \frac{P_c}{\rho_c^2} \left( \frac{\partial \rho}{\partial \mu} \right)_T = \frac{P_c}{\rho_c^2 g} \frac{d\rho}{dz} \quad (7)$$

is obtained from our data by measuring the spacing  $dz$  of the interference fringes corresponding to density difference  $d\rho$  closest to the middle of the cell, where the

TABLE I. Coexistence curve fits. Fits 1 and 2, temperature interval  $10^{-6} < -t < 10^{-4}$ ; fits 3–7, temperature interval  $10^{-6} < -t < 4.2 \times 10^{-4}$ . Exponent values in parentheses were kept fixed for the fit.

Fit	$\beta$	$\Delta$	$B_0$	$B_1$	$B_2$	$B_3$
1	(0.327)	(0.5)	1.744	0.94		
2	0.3282	(0.5)	1.765	0.82		
3	(0.325)	(0.5)	1.717	0.96	-1.85	
4	(0.327)	(0.5)	1.747	0.85	-1.59	
5	0.3310	(0.5)	1.806	0.64	-1.08	
6	(0.327)	(0.5)	1.739	1.03	-3.39	5.3
7	0.3287	(0.5)	1.770	0.85	-2.34	2.9

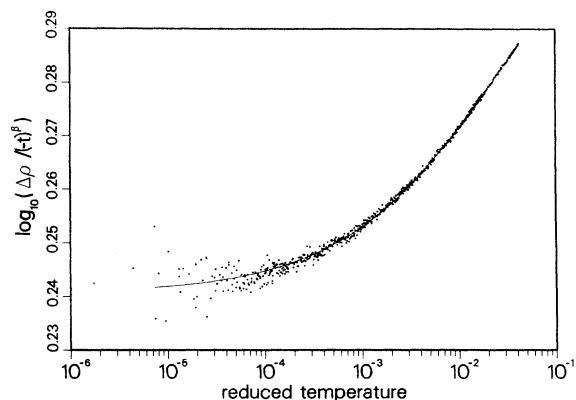


FIG. 2. Sensitive log-log plot of coexistence curve data as a function of reduced temperature. The curve corresponds to a fit with three correction to scaling terms and with the critical exponents fixed at  $\beta = 0.327$  and  $\Delta = 0.5$ .

gradient of the density profile is highest and thus the compressibility is largest. Figure 3 shows a plot of compressibilities in both the one and two phase regions.

In the one phase region, a least-squares fit of the logarithm of  $\kappa_T^+$  as a function of the logarithm of  $t$  (shown in the figure) yields an exponent  $\gamma^+ = 1.230(8)$  and a critical amplitude  $\Gamma_0^+ = 0.058(3)$ . The critical temperature was

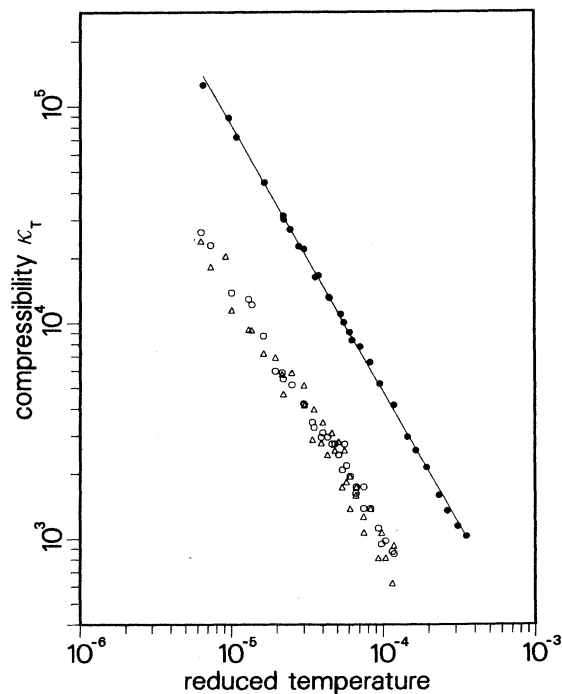


FIG. 3. Compressibility results. The data for  $T < T_c$  (two-phase region) are represented by open circles (vapor phase) and open triangles (liquid phase). Data in the one phase region ( $T > T_c$ ) are represented by solid circles, and the curve is a power-law fit to them, with exponent  $\gamma = 1.230$ .

TABLE II. Compressibility fits. Exponent values shown in parentheses were kept fixed for the fit.

	$\gamma^+$	$\Gamma_0^+$
$T > T_c$	$1.230 \pm 0.008$	$0.058 \pm 0.005$
one-phase region	(1.23)	$0.058 \pm 0.003$
	(1.24)	$0.052 \pm 0.002$
	$\gamma^-$	$\Gamma_0^-$
$T < T_c$	$1.18 \pm 0.03$	$0.019 \pm 0.008$
two-phase region	(1.23)	$0.012 \pm 0.002$
	(1.24)	$0.011 \pm 0.001$

determined as a free parameter and found to agree with the value found from the fit of the coexistence curve to within 0.2 mK. The figure shows that the straight line is sufficient to describe the data. Correction to scaling terms in this temperature range would be of the order of 1% and cannot be discriminated from the statistical scatter of the data.

In the two-phase region, data extraction is much more difficult, due to a lower curvature of the interference pattern, and thus the data in this region are somewhat more scattered. A two-parameter fit for  $T < T_c$ , for which the critical temperature was kept fixed at the value found in the one-phase region, yields  $\gamma^- = 1.18(3)$ , which is substantially lower than the theoretical value ( $\gamma^- = \gamma^+ = 1.24$ ). In order to obtain information on the critical amplitudes,  $\Gamma_0^\pm$ , data in both regions were fitted by power laws with  $\gamma = 1.23$  (corresponding to the exponent in the one-phase region) and  $\gamma = 1.24$  (the theoretical value). For these fits, the critical temperature was held fixed at the value found in the coexistence curve fit. The results of these fits are summarized in Table II.

### C. Critical isotherm

In order to extract the critical amplitude  $D_0$  of the critical isotherm, we follow the approach suggested by Pestak and Chan.<sup>13</sup> At temperatures close to  $T_c$  the distance  $\Delta z$  of several interference fringes from the meniscus was measured. Then, for each temperature, the quantity

$$D_t = \frac{P - P_c}{P_c (\Delta\rho^*)^\delta} = \frac{\rho_c g}{P_c} \frac{\Delta z}{(\Delta\rho^*)^\delta} \quad (8)$$

was calculated for the reduced density

$$\Delta\rho^* = |\rho(\Delta z) - \rho_c| / \rho_c$$

corresponding to this fringe. The value of  $\delta$  was determined using the scaling relation  $\gamma = \beta(\delta - 1)$  and the values of  $\gamma$  and  $\beta$  determined earlier in the same experiment. On the critical isotherm, all the values of  $D_t$  thus calculated should coincide (this will give the value of the critical amplitude  $D_0$ ). However, for data taken at temperatures away from  $T_c$ , the functional relation  $\Delta\mu = D_0 |(\rho - \rho_c) / \rho_c|^\delta$  is not precisely fulfilled. Below  $T_c$ , the density profile is "steeper" than on the critical isotherm and thus the values of  $D_t$  as calculated from formula (8) are smaller than the critical value  $D_0$ . At any given temperature  $T < T_c$ , the values of  $D_t$  decrease with increasing distance  $\Delta z$  from the meniscus. Above  $T_c$ , the

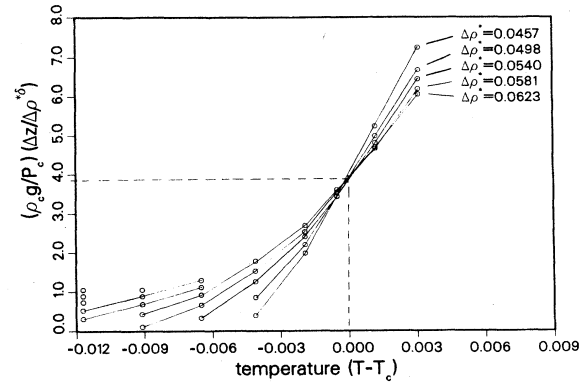


FIG. 4. Example of the graphical method used for extracting the amplitude of the critical isotherm. The lines correspond to fringes with a fixed density difference  $\Delta\rho^*$  from the critical density. The lines intersect at the critical temperature; this intersection determines the critical amplitude  $D_0$ .

density profile is "less steep", and therefore the  $D_t$  values are larger than  $D_0$ .

In order to assure that gravitational rounding does not play an appreciable role, only data with  $\Delta\rho^* > 4 \times 10^{-2}$  were taken into account for which beam-bending errors are less than 0.1%.<sup>17</sup> A symmetrical density profile was assumed, and the  $\Delta z$  used for the evaluation was the mean of the vapor and liquid values. The data of one run (with  $\delta = 4.80$ ) are shown in Fig. 4. As can be seen, lines corresponding to various values of  $\Delta\rho^*$  indeed do intersect at the critical temperature, and this furnishes the amplitude  $D_0$ . Using  $\delta = 4.76$  (corresponding to  $\beta = 0.327$ ,  $\gamma = 1.23$ ), one obtains  $D_0 = 3.5 \pm 0.2$ , whereas for  $\delta = 4.80$  (corresponding to  $\beta = 0.327$ ,  $\gamma = 1.24$ ), one obtains  $D_0 = 3.85 \pm 0.3$ .

### D. Critical temperature

For each run, the critical temperature was determined in three different ways: from a least-squares fit to the coexistence curve data, from a power-law fit to the one phase compressibility, and from the intersection of  $D_t$  lines belonging to different densities near the critical isotherm. The three values of  $T_c$  thus obtained agree to within 0.2 mK, which indicates that the results for the critical amplitudes are quite self-consistent.

Data were taken over a period of about 8 months. During this time, the critical point shifted steadily at a rate of  $\approx 4$  mK/month. This may be due to a reaction of the fluoroform with the indium seals of the cell or a slow "outgassing" from the cell walls or windows.<sup>6</sup> Within experimental error, this drift does not affect the critical amplitudes. It has been corrected for when evaluating several data sets together.

## IV. DISCUSSION

Table III presents a collection of the various critical amplitudes from fits with different critical exponents and Table IV shows the corresponding values of the critical amplitude ratios. The experimental values are in good agreement with theoretical predictions,<sup>11</sup> independent of

TABLE III. Critical amplitudes of fluoroform. Exponent values in parentheses were kept fixed for the fit.

$\beta$	$\gamma$	$\delta$	$B_0$	$\Gamma_0^+$	$\Gamma_0^-$	$D_0$
(0.327)	(1.23)	(4.76)	1.743±0.003	0.058±0.003	0.012±0.002	3.5±0.2
(0.327)	(1.24)	(4.80)	1.743±0.003	0.052±0.002	0.011±0.001	3.85±0.30
(0.325)	(1.23)	(4.79)	1.722±0.003	0.058±0.003	0.012±0.002	3.75±0.30
(0.325)	(1.24)	(4.82)	1.722±0.003	0.052±0.002	0.011±0.001	4.1±0.3

the precise values of exponents one chooses for the fits. There is excellent agreement between the amplitude ratios obtained by different choices of the critical exponents. Our results are not accurate enough, however, to decide whether high-temperature series expansions or  $\epsilon$  expansions yield the better values of the ratios.

We also find good agreement with the results of Pestak and Chan<sup>13</sup> from measurements on N<sub>2</sub> and Ne. For the amplitude ratio  $D_0\Gamma_0^+B_0^{\delta-1}$  the uncertainty in our results is lower than theirs due to the fact that close to the critical point, their data are strongly influenced by gravitational rounding which causes a large error in the amplitude  $D_0$ . Our experiment, being less affected by gravitational rounding errors, determines  $D_0$  to much higher accuracy, resulting in a more precise value of the amplitude ratio.

In order to check the self-consistency of our data, the critical temperature was determined separately from fits to the coexistence curve and compressibility data and from the intersection of the lines of constant density as used for the evaluation of the critical isotherm. The values of  $T_c$  obtained by these three different methods agree to within 0.2 mK. A discrepancy of the  $T_c$  values can be an indication of gravitational rounding or insufficient equilibration time between temperature steps. We thus conclude that our data are to a large extent free of these errors.

Also, capillary effects do not play an appreciable role in this system; they would manifest themselves as a smearing out of the meniscus separating the liquid and the vapor phase. On our films, the meniscus is always very narrow, which indicates that there is negligible wetting of the sapphire windows, even far from the critical point.

TABLE IV. Critical amplitude ratios

	$\Gamma_0^+/\Gamma_0^-$	$D_0\Gamma_0^+B_0^{\delta-1}$
Our data		
( $\beta=0.327$ , $\gamma=1.23$ )	4.8±0.6	1.64±0.12
( $\beta=0.327$ , $\gamma=1.24$ )	4.8±0.6	1.61±0.14
( $\beta=0.325$ , $\gamma=1.23$ )	4.8±0.6	1.70±0.14
( $\beta=0.325$ , $\gamma=1.24$ )	4.8±0.6	1.69±0.14
Pestak <i>et al.</i>		
N <sub>2</sub>	4.8±0.6	1.71±0.5
Ne	4.8±0.8	2.05±0.8
Theory		
high-temperature series	5.07	1.75
$\epsilon$ expansion	4.80	1.6

A more subtle point is the behavior of the Lorenz-Lorentz function close to the critical point. Both density and refractive index have been predicted to have an inherent critical anomaly,<sup>21,22</sup> both with the same exponent, which makes it difficult experimentally to distinguish between the two phenomena. We observe a weak critical anomaly in the density close to  $T_c$ ,<sup>18</sup> of the same order of magnitude as observed in other experiments on nonpolar substances.<sup>23</sup> No definite experimental evidence exists for the anomaly of the refractive index at optical frequencies.<sup>24</sup> Our method of determining the Lorenz-Lorentz function does not allow us to perform precise measurements close to  $T_c$  (Ref. 18) which would detect such an anomaly. We therefore have to assume  $\mathcal{L}$  in Eq. (5) to be a constant in the critical region.

The compressibility data do not extend far enough away from  $T_c$  to detect any deviations from pure power-law behavior, but the evaluation of the coexistence curve clearly shows the importance of correction-to-scaling terms. Even though three correction terms are sufficient to describe the data in the temperature interval  $10^{-6} < -t < 2 \times 10^{-2}$ , the large variations in the amplitudes  $B_2$  and  $B_3$  from fit to fit indicate that using a power series for the evaluation is not satisfactory any more, and that the data should instead be evaluated using crossover theories.<sup>25,26</sup> However, when both  $\beta$  and  $\Delta$  are kept fixed at their theoretically expected value, the amplitude  $B_0$  changes very little (by less than 0.5%) when more correction-to-scaling terms are included. Thus the leading critical amplitude can be reliably extracted independent of the exact behavior of the coexistence curve far from critical.

The absolute value of the critical amplitude  $B_0$  is considerably higher than the ones measured for nonpolar gases,<sup>27,28,13,29</sup> whereas  $D_0$  is appreciably lower.<sup>13</sup> This is probably due to the fact that fluoroform, being a polar gas, is not expected to obey the "principle of corresponding states" as well as nonpolar fluids do.<sup>30</sup> The same trend has also been observed for H<sub>2</sub>O and D<sub>2</sub>O.<sup>25</sup> It is in accord with the theory of scaling, however, that polar fluids, even though deviating in the absolute values of their critical amplitudes, still furnish the same amplitude ratios as nonpolar ones.

#### ACKNOWLEDGMENTS

We would like to thank J. R. de Bruyn and D. S. Zimmerman for helpful discussions and for a critical reading of the manuscript. This work was supported by the National Sciences and Engineering Research Council of Canada.

- <sup>1</sup>M. J. George and J. J. Rehr, *Phys. Rev. Lett.* **53**, 2063 (1984).
- <sup>2</sup>J.-H. Chen, M. E. Fisher, and B. G. Nickel, *Phys. Rev. Lett.* **48**, 630 (1982).
- <sup>3</sup>J. C. LeGuillou and J. Zinn-Justin, *Phys. Rev. B* **21**, 3976 (1980).
- <sup>4</sup>Bernie Nickel and Mark Dixon, *Phys. Rev. B* **26**, 3965 (1982).
- <sup>5</sup>K. E. Newman and E. K. Riedel, *Phys. Rev. B* **30**, 6615 (1984).
- <sup>6</sup>R. Hocken and M. R. Moldover, *Phys. Rev. Lett.* **37**, 29 (1976).
- <sup>7</sup>F. J. Wegner, *Phys. Rev. B* **5**, 4529 (1972).
- <sup>8</sup>J. Adler, M. Moshe, and V. Privman, *Phys. Rev. B* **26**, 3958 (1982).
- <sup>9</sup>B. Widom, *J. Chem. Phys.* **43**, 3898 (1965).
- <sup>10</sup>H. Güttinger and D. S. Cannell, *Phys. Rev. A* **24**, 3188 (1981).
- <sup>11</sup>A. Aharony and P. C. Hohenberg, *Phys. Rev. B* **13**, 3081 (1976).
- <sup>12</sup>L. A. Weber, *Phys. Rev. A* **2**, 2379 (1970).
- <sup>13</sup>M. W. Pestak and M. H. W. Chan, *Phys. Rev. B* **30**, 274 (1984).
- <sup>14</sup>M. W. Pestak, Ph.D. thesis, Pennsylvania State University, 1983.
- <sup>15</sup>P. Schofield, *Phys. Rev. Lett.* **22**, 606 (1969).
- <sup>16</sup>J. T. Ho and J. D. Litster, *Phys. Rev. B* **2**, 4523 (1970).
- <sup>17</sup>M. R. Moldover, J. V. Sengers, R. W. Gammon, and R. J. Hocken, *Rev. Mod. Phys.* **51**, 79 (1979).
- <sup>18</sup>U. Nürger and D. A. Balzarini, *Phys. Rev. B* (to be published).
- <sup>19</sup>D. A. Balzarini, *Can. J. Phys.* **50**, 2194 (1972).
- <sup>20</sup>See AIP document No. PAPS PRBMDO-39-9330-21 for 21 pages of these data. Order by PAPS number and journal reference from American Institute of Physics, Physics Auxiliary Publication Service, 335 East 45th Street, New York, NY 10017. The prepaid price is \$1.50 for a microfiche (98 pages), or \$5.00 for photocopies of up to 30 pages. Airmail additional. Make checks payable to the American Institute of Physics.
- <sup>21</sup>S. Y. Larson, R. D. Mountain, and R. Zwanzig, *J. Chem. Phys.* **42**, 2187 (1965).
- <sup>22</sup>R. Hocken and G. Stell, *Phys. Rev. A* **8**, 887 (1973); G. Stell and J. S. Hoye, *Phys. Rev. Lett.* **33**, 1268 (1974).
- <sup>23</sup>M. W. Pestak, R. E. Goldstein, M. H. W. Chan, J. R. de Bruyn, D. A. Balzarini, and N. W. Ashcroft, *Phys. Rev. B* **36**, 599 (1987).
- <sup>24</sup>J. V. Sengers, D. Bedeaux, P. Mazur, and S. C. Greer, *Physica* **104A**, 573 (1980).
- <sup>25</sup>J. V. Sengers and J. M. H. Levelt-Sengers, *Annu. Rev. Phys. Chem.* **37**, 189 (1986).
- <sup>26</sup>P. C. Albright, J. V. Sengers, J. F. Nicoll, and M. Ley-Koo, *Int. J. Thermophys.* **7**, 75 (1986).
- <sup>27</sup>O. G. Mouritsen, D. Balzarini, and P. Palffy, *Can. J. Phys.* **61**, 1301 (1983).
- <sup>28</sup>D. Balzarini and O. G. Mouritsen, *Phys. Rev. A* **28**, 3515 (1983).
- <sup>29</sup>J. R. deBruyn and D. A. Balzarini, *Phys. Rev. A* **36**, 5677 (1987).
- <sup>30</sup>E. A. Guggenheim, *Thermodynamics* (North-Holland, Amsterdam, 1967).